STUDIA UBB CHEMIA, LVI, 4, 2011 (p. 169 - 180)

NUMERICALLY MODELLING THE O_3/UV ADVANCED OXIDATION REACTORS BY USING THE COMPUTATIONAL FLUID DYNAMICS METHOD

SORIN CLAUDIU ULINICI[a,*], GRIGORE VLAD[a], BOGDAN HUMOREANU[a], SIMION AŞTILEAN[b]

ABSTRACT. The O_3/UV advanced oxidation processes constitute physical-chemical processes recently used as efficient processes of degrading the organic substances and for disinfection purposes within the water treatment and purging technologies. Technically speaking, the O_3/UV advanced oxidation systems involve two kinds of distinct processes: the gas/liquid (O_3/aqueous solution) transfer, which is a distinct physical step, and the transfer of the ultra-violet radiation photons transfer (λ<310 nm) into the solution and the initiation of a chain of reactions leading both to direct photodegradation processes and to highly reactive OH^o radicals species generation processes. This work suggests the elaboration of a numerical template for the advanced oxidation reactors (O_3/UV) based on the CFD (Computational Fluid Dynamics) method, by using the FEM (Finite Element Method) for numerically solving the differential equations systems. This template may constitute both the basis for the elaboration of designing methods in the field of water treatment equipment engineering and the modelling basis for studying more complex advanced oxidation systems, which include heterogeneous photocatalysis processes.

Keywords: *Computational Fluid Dynamics, advanced oxidation, numerical modeling, ozone photolysis*

INTRODUCTION

The classical procedures of removing micro-pollutants from water, and the disinfection processes involve the utilisation of certain oxidising agents or of certain physical agents that generate the degradation of theses pollutants. It is about processes that use the chlorine freed by various compounds thereof, by the ozone or peroxide oxidation or by the UV radiation action. All these procedures, applied separately, have disadvantages linked to slow degradation (or to the absence of degradation) in case of certain compounds, or to the generation of certain secondary reaction compounds (such as the trihalomethanes – in case of the chlorine utilisation). It is in this

[a] S.C. ICPE Bistrita S.A., Str. Parcului, Nr.7, RO-420035 Bistrita, Romania, **sorin_ulinici@icpebn.ro*
[b] Babes-Bolyai University, Faculty of Physics, Institute for Interdisciplinary Research in Bioanoscience, Nanobiophotonics Center, T. Laurian 42, 400271 Cluj-Napoca, Romania

context that the necessity of developing new highly yielded and highly efficient degradation and mineralisation (in case of the organic substances) unselective physical-chemical processes have appeared [1]. The advanced oxidation processes (AOP) fall into this category, as they have been intensively studied and investigated this last decade [11].

The advanced oxidation processes are deemed to be those processes that lead to the oxidative, unselective and energetic degradation of the organic and inorganic substances in the presence of the highly reactive OH^o radical species. These processes are physical-chemical ones, which include both the OH^o radicals generation stage and the reaction products reaction and removal steps. There is a whole diversity of physical and chemical processes that lead to the generation of the OH^o free radicals in an aqueous environment. We can talk about the action of the low temperature plasmas (cold plasmas), about processes of decomposing the O_3 in an aqueous environment, catalytic ozonisation processes [3], advanced oxidation processes in O_3/UV (the ozone photolysis) [7], H_2O_2/UV, H_2O_2/O_3, H_2O_2/O_3/UV systems, about Fenton processes, heterogeneous photocatalysis processes, about the electro-hydraulic cavitation and sonolysis, about processes of super-critically oxidising water, about the action of the γ radiation and of the cathode beams. The use of the advanced oxidation processes for water treatment involve both scientifically knowing the involved phenomena and mechanisms and the capability of designing and implementing such processes at a real scale. In this context, this work here approaches, from the theoretical standpoint and from the numerical modelling one, the O_3/UV advanced oxidation processes in photolysis reactors, this approach being a continuation of certain previous steps related to the modelling of the O_3/UV advanced oxidation systems by using numerical templates elaborated in conformity with certain software environments strictly dedicated to the hydraulic systems, by using experimental data obtained by the exploitation of a pilot station [16]. The numerical modelling involved the use of concepts and methods taken from Computational Fluid Dynamics (**CFD)**, by using the Navier-Stokes equation systems, combined with physical and chemical templates linked to processes of energetically transferring the UV radiation, to convection, diffusion and reaction [17]. The finite element method (FEM) was used for solving the equation systems with partial differentials and limit conditions [15], with an aim to depict the physical and chemical phenomena involved, by using the **Comsol Multiphysics 3.5** software environment [5] .

RESULTS AND DISCUSSION

The physical and numerical template of the advanced oxidation (O_3/UV) reactor

The use of the UV reactors within the O_3/UV advanced oxidation processes involve knowing and exploiting their characteristics, so that maximum yields may be reached under reasonsable energetic consumptions. The use

of the O_3/UV reaction systems for water treatment involves two categories of processes: photo-chemical degradation and photolysis processes and direct disinfection processes.

If the disinfection processes involve the maintenance of a certain contact time between the water flow subjected to the process and the UV radiation field (the provision of a minimum energetic dose, expressed in J/m^2), in case of the photo-chemical degradation processes, what is relevant is the intensity of the radiation field and the profile of the concentrations in the initial condition and in the equilibrium condition, with the help of the reactor, of the chemical species that are of interest, in our case of ozone. A high rate of ozone photolysis involves reaching a high level of the instantaneous concentrations of OH^o radicals. The global reaction rate for the ozone photolysis process is pro rata the product between the quantic yield of the photolysis reaction and the energy of the UV radiation absorbed in the time unit and in the volume unit, according to the following relation [2], [14]:

$$\frac{d[O_3]}{dt} = -\Phi_{O_3} \cdot W_\lambda \tag{1}$$

where

$[O_3]$ – the concentration of the dissolved oxygen $[mol/m^3]$

Φ_{O3} – the quantic yield of the photolysis process [mol/J]

W_λ – the volume density of the absorbed power for the wavelength radiation λ $[W/m^3]$

The volume density of the absorbed power can be put down as :

$$W_\lambda = \mu I_\lambda = 2.303 \cdot \left(\varepsilon_{O_3} C_{O_3} + \sum_i \varepsilon_i C_i\right) \cdot I_\lambda \tag{2}$$

where : μ – the attenuation coefficient [1/m]; ε_i – the coefficient of absorbing the i species to the λ wavelength (mol^{-1}. m^{-1}); I_λ – the energetic intensity of the radiation in that respective point, at the λ wavelength $[W/m^2]$.

Equation (2) characterises the density of the power absorbed by all the chemical species present in the solution that have absorption band to the λ wavelength. If we strictly refer to the ozone photolysis process, we may introduce the fraction of the density of power absorbed by the ozone, by using the following expression :

$$F_{O_3} = \frac{\varepsilon_{O_3} C_{O_3}}{\sum_i \varepsilon_i C_i} \tag{3}$$

The ozone photolysis process rate can be written down as :

$$\frac{d[O_3]}{dt} = -\Phi_{O_3} \cdot F_{O_3} . I_\lambda \tag{4}$$

The numerical modelling of the photolysis process involves knowing the spatial distribution of the radiation's energetic intensity. The great majority of the industrial UV reactors have a coaxial configuration, with the UV lamp placed inside a quartz cylindrical casing, acording to Figure 1 (the annular reactor).

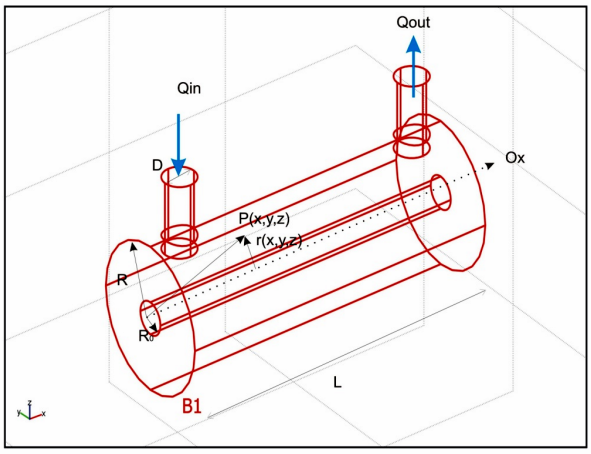

Figure 1. The typical configuration of an O_3/UV annular reactor

There are three basic mathematical templates that describe the spatial distribution of the energetic intensity sent out by the cylindrically shaped lamp [5], [10], [12-13]: the LL template – based on the Lambert law, the PSSE (Point Source with Spheric Emission) template, where the UV lamp is shaped by means of a series of co-linear points, which release an energy spherical spatial distribution, and the LSPP (Linear Source with emission in Parallel Planes) template, according to which the lamp sends out equal energetic intensities in planes that are parallel to the lamp axis. The classic methods of modelling the UV reactors are based on the use of certain global parameters, on the reaction configuration (the effective path of radiation), and on particulars of the geometrical system and of the UV source irradiance characteristics, generally determined by actinometric experimental methods. The main disadvantages of the classic approach relate to the impossibility of extending the templates for more complex geometrical configurations, the global treatment of the reaction system, the impossibility of modelling dynamic regimes. The template presented in this work wipes off the aforesaid disadvantages, constituting the premise of the theoretical and practical approach of complex configurations for the O_3/UV reaction systems.

The template hypotheses:

1. The modelling of the energetic intensity's spatial distribution was made according to the LSSP template, because of its simplicity and of the possibility

of the numerical implementation. According to this template, the radiation energetic implementation is described by the following equation [2], [10]:

$$I = I_0 \frac{r_0}{r(x,y,z)} e^{-(r(x,y,z)-r_0)} \tag{5}$$

where :

r_0 – the interior radius of the UV reactor (the radius of the quartz casing)
r(x,y,z) – the distance from the lamp to the P point (x,y,z)
I_0 – the irradiance (the energetic intensity) sent out by the lamp [W/m^2]

2. The fluid flow is the flow of an incompressible fluid, so that the Navier-Stokes equations for incompressible fluids (ρ_m= constant) stand valid for the flowing area of the reactor, according to the system of equations written for the 3 axes of coordinates [4] :

$$\rho_m \frac{du_i}{dt} = -\frac{\partial p}{\partial x_i} + \mu \nabla^2 u_i + \rho_m g_i \quad i = 1 \dots 3 \tag{6}$$

where ρ_m is the mixture density, u_i is the field of speeds in the fluid, g_i represents the components on the three axes of the gravitational acceleration and μ is the volume dynamic viscosity.

2. The reaction kinetics is governed by the two basic equations : the reaction rate equation (4) and the mass transport equation (the non-conservative convection-diffusion equation), the reaction rate being the one specified above (Eq.4) :

$$\frac{\partial c_{O_3}}{\partial t} + \nabla \cdot (-D \nabla c_{O_3}) = R - \nabla \cdot (c_{O_3} \vec{u}) \tag{7}$$

where c_{O3} is the concentration of the ozone dissolved in water in each point of the volume field taken into consideration and D is the turbulent diffusion coefficient of the ozone solubilised in the fluid environment.

3. The water flow uppon the entrance in the reactor is constant, having a constant value of the dissolved ozone concentration.

4. The fluid flow is attached a template of turbulent flow k-ε [5], [9].

The geometry of the O_3/UV advanced oxidation reactor

One has selected two particular geometries, which correspond one to another in practice from the viewpoint of the geometrical characteristics, of the flow parameters and of the functional parameters of the UV radiation source. In case of the template of the reactor with a longitudinal flow with one UV radiation coaxial source (Figure.1), the basic parameters taken into consideration are presented in Table 1.

Table 1. The value of the basic parameters for the longitudinal reactor

The geometrical/functional parameter	**Value**
The active length of the generator L [m]	0.50
The exterior radius of the reactor R [m]	0.10
The interior radius of the reactor R_0 [m]	0.0225
The diameter of the entrance/exit joint D [m]	0.05
The water flow rate Qin [m^3/h]	10
The irradiance of the UV lamp in the 254 nm line [mW/cm^2] (at the level of the quartz casing)	68.00
The concentration, upon the entrance in the reactor, of the dissolved ozone [g/m^3]	1.00

Figure 2 presents the configuration of the reactor with crosswise circulation and 2 sources of UV radiation that are parallel to the reactor axis. The main parameters of the template are displayed in Table 2.

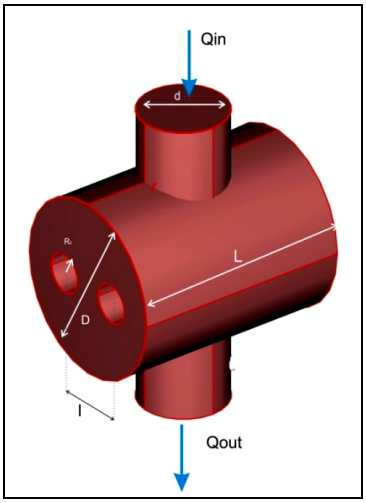

Figure 2. The geometry of the O_3/UV reactor in a crosswise configuration

Table 2. The value of the basic parameters for the crosswise reactor

The geometrical/functional parameter	**Value**
The active length of the generator L[m]	0.250
The exterior radius of the reactor R [m]	0.100
The interior radius of the reactor R_0 [m]	0.0225
The distance between the radiation sources axes l(m)	0.080
The water flow rate Qin [m^3/h]	100
The irradiance of the UV lamp in the 254 nm line [mW/cm^2]	269
The concentration, upon the entrance in the reactor, of the dissolved ozone [g/m^3]	1.00

The modelling of the advanced oxidation reactors was performed by using the finite elements method (FEM), in the Comsol Multiphysics 3.5. software environment.

The values of the physical constants taken into account for both configurations are displayed in Table 3.

Table 3. The constants of the CFD template

Constant / Characteristic	Value
The fluid temperature [K]	293
The molar absorbance of ozone in water ε [m^2/mol]	330
The quantic yield at 254 nm Φ_{254} [m^2/mol]	$0.1322 \cdot 10^{-5}$
The molar mass of O_3 [g/mol]	47.98
The coefficient of diffusion of ozone in water D [m^2/s]	$2.29 \cdot 10^{-9}$
The water dynamic viscosity η [Pa·s]	10^{-3}
The water absorption coefficient at 254 nm α [m^{-1}]	10

The results analysis and interpretation

The numerical modelling mainly aimed at assessing the ozone photolysis reaction rate in the reactor and at assessing the concentrations of dissolved ozone in various points of the reactor's volume and upon the exit therefrom. The parametrical assessment of the reaction rate and of the dissolved ozone concentration, if the ozone flow rate and concentration are constant upon entrance, was made subject to the values of the UV lamps irradiance I_0[mW/cm^2].

The reactor with a longitudinal circulation. Figure 3 presents the modelling results for the longitudinal distributions of the fluid velocity in the reactor. We find that the values of the velocity components on the y and z axes at the given time are both positive and negative, with fluctuations along the longitudinal axis at the level of the quartz casing. The velocity component on the x axis is positive throughout the whole range and negative values are only recorded at the frontier of axis Ox of the reactor, due to the 'reflexion' to the wall thereof, which brings forth a quasi-stationary area. As compared to the velocities recorded in the reactor's admission and evacuation area (> 1.5 m/s), the fluid's running speed in the quartz casing area is relatively low.

The profile of the reaction rate in various radial sections of the reactor (z = 3;5;8;10 cm), depending on the x quota, shows a dramatic diminishment of the same and an increase of the radial distance to the quartz casing, the value of the reaction rate having a decreasing evolution along the Ox axis, which is mainly due to the diminishment of the dissolved ozone concentration (Figure 4).

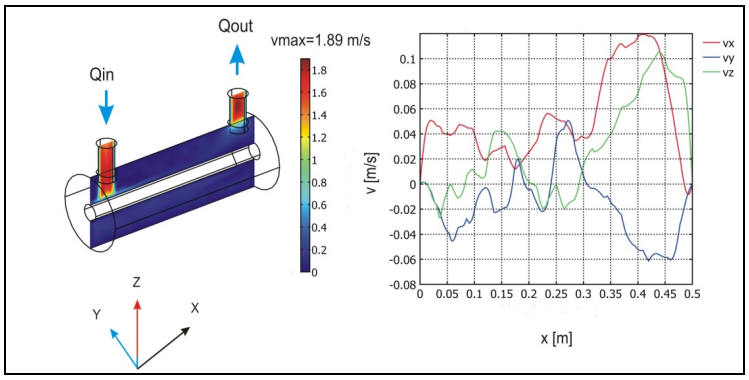

Figure 3. The longitudinal velocity distribution

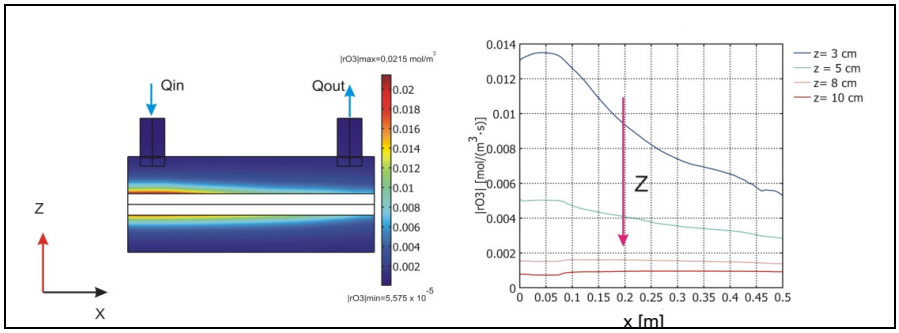

Figure 4. The longitudinal profile of the reaction rate

The variation in the longitudinal plane of the dissolved ozone concentrations is rendered in Figure 5, for various z quotas. The parametrical dependance on the value of the I_0 radiance of the UV lamp for the mean reaction volume rate and the ozone concentration upon the exit from the reactor is given in Figure 6. The analysis of the concentration profiles shows an abrupt drop on the x coordinate, with a maximum peak for positive values of z (due to the entrance joint), and a smoother evolution for the negative values of z.

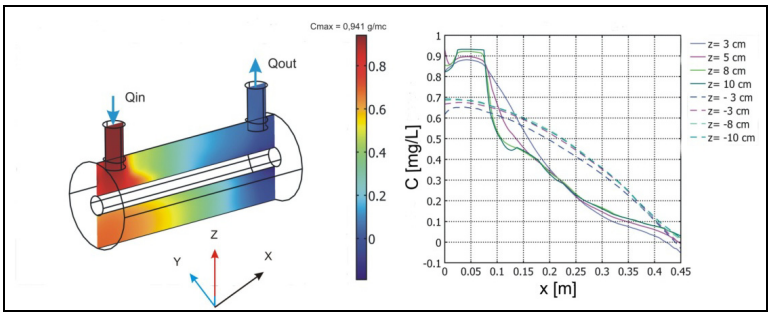

Figure 5. The distribution of the ozone concentrations on the longitudinal axis

Even though the theoretical ozone concentration upon entrance is $1gO_3/m^3$, because of the 'flow'-type frontier condition ($gO_3/m^2 \cdot s$), the maximum value of the concentration is 0.941 gO_3/m^3, which is due to the extension of the reaction field including at the level of the reactor entrance joint.

The parametrical analysis depending on the lamp irradiance value [$I_0(mW/cm^2)$] is displayed in Figure 6 and Figure 7. The reaction rate increases at the same time with the enhancement of the irradiance value, the O_3 concentration dropping at the same time with this increase.

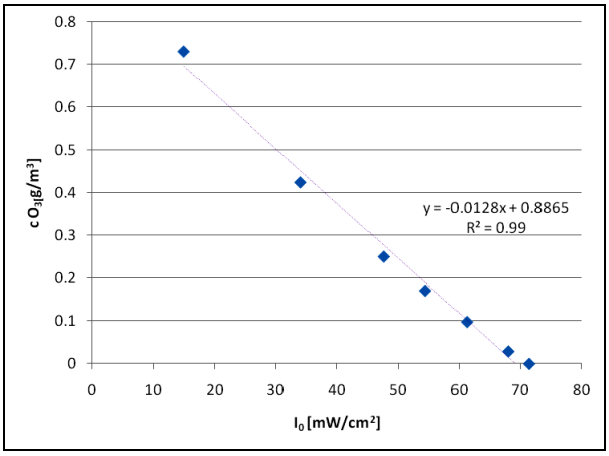

Figure 6. The parametrical variation of the ozone concentration upon the exit from the reactor

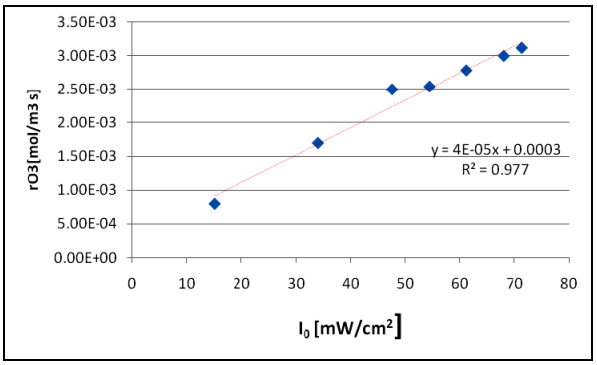

Figure 7. The parametrical variation of the average volume reaction rate

In case of the constructive crosswise-type reactor, the module enables the approach of fluid flow rates upon the entrance in the system that are considerably higher than in case of the longitudinal-type reactor. The distribution of the speeds in the system enables the appearance of 'stagnant' areas, with a reduced fluid speed at the longitudinal extremities and at the reactor's external radius quota. One notices (Figure 8) high values of the fluid velocity

recorded in the median area located between the two quartz tubes. The reaction rate, r_{O3}, is tightly correlated to the intensity of the UV radiation and to the field of speeds in the reactor, showing a minimum value in the central area, with high values of the speeds and maximum values in the other areas. The longitudinal profile of the O_3 concentrations shows a maximum value in the central areas and a lower efficiency of the photolysis process in these regions (Figure 9a).

Upon the exit from the system, the maximum value decreases and the curve profile narrows. The concentrations profile can be best noticed in case of the central section, the maximum area becoming increasingly narrow upon the exit from the reactor (Figure 9b). The blue colour corresponds to areas with a maximum efficiency of the photolysis process. The longitudinal profiles of ozone concentrations are depicted in Figure 10.

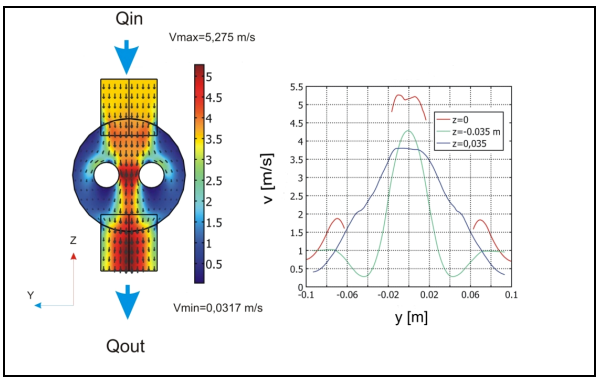

Figure 8. The velocity distribution in the crosswise section for the crosswise-type 2- lamped reactor

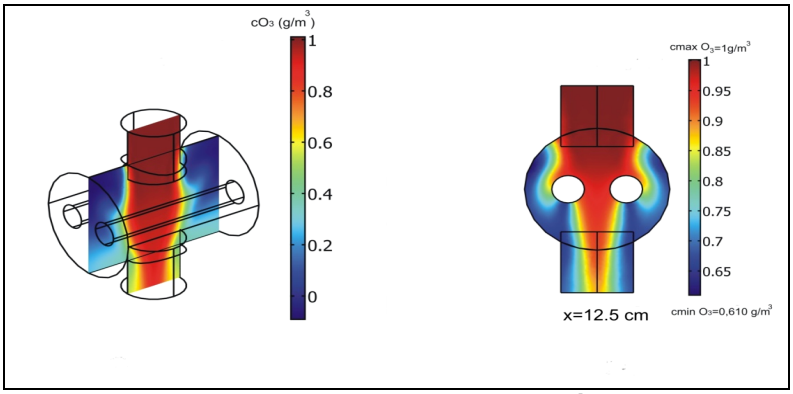

a. **b.**

Figure 9. The ozone concentrations distribution: a) In the longitudinal plane; b) In the crosswise plane

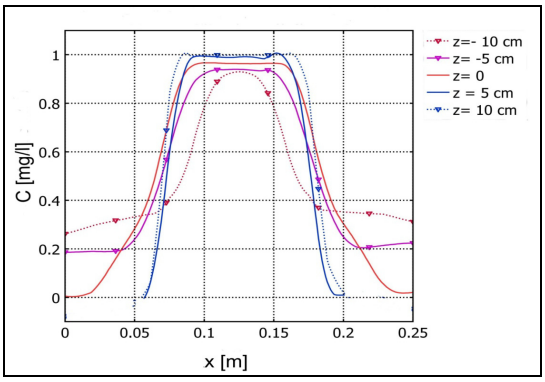

Figure 10. The longitudinal profile of the ozone concentrations

The parametrical analysis depending on the UV radiance of a lamp shows, like in case of the longitudinal template, a quasi-linear dependance of the concentrations upon the exit from the reactor (Fig. 11), a similar dependance being also recorded in case of the average volume reaction rate.

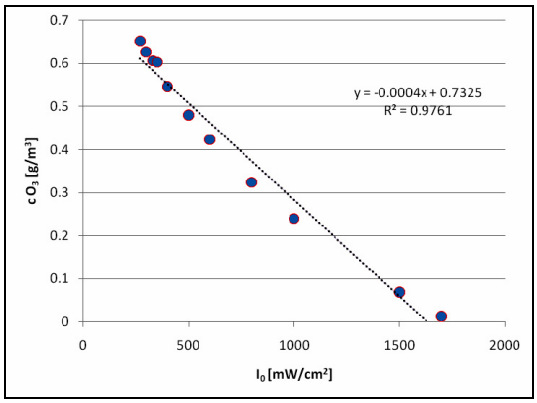

Figure. 11. The parametrical variation of the ozone concentration upon the exit from the reactor depending on the lamp irradiance

CONCLUSIONS

The modelling of the O_3/UV advanced oxidation reactors by using the CFD method brings along higher strictness in the rigorous approach of the ozone photolysis step. If systems of differential equations with partial Navier-Stokes derivates and convection-diffusion ones in the geometrical field of the reactor, combined with a template of distribution of the UV radiation intensity in its volume are used, highly accurate predictions on the photolysis reaction rates and the ozone concentrations from and upon the exit from the reactor can be obtained.

In case of each point of the reactor, the possibility of reaching the basic sizes involved (the speeds components, the radiation intensity, the reaction rate, the ozone concentration) and the possibility of reaching mediated global values for the reaction rates, concentrations and the fluid residence time enable the elaboration of extremely efficient engineering design instruments.

From the standpoint of the research activities, the use of this method for modelling the O_3/UV advanced oxidation reactors enables the extension of the template for various geometries of reactors, with the possibility of including new components and physical and chemical mechanisms in the system, linked to photocatalysis, catalytic ozonisation, sonolysis and electro-chemical separation.

ACKNOWLEDGMENTS

This work has been supported by National Authority for Scientific Research (ANCS) through programme INNOVATION grant no. 177/2008: 'Installation to obtain ultrapure water out of primary sources'.

REFERENCES

1. R. Andreozzi, V. Caprio, A. Insola, R. Marrota, *Catalysis Today*, **1999**, *53:1,* 51.
2. F.J. Beltrán, *Ozone: Science & Engineering*, **1997**, *19:1*, 13.
3. F.J. Beltrán, „Ozone Reaction Kinetics for Water and Wastewater Systems", Lewis Publishers, London, N.Y, **2004**.
4. J. Blazek, "Computational Fluid Dynamics: Principles and Applications, Elsevier Science Ltd., **2001**.
5. Comsol Inc., "Chemical Engineering Module User's Guide", Comsol AB, **2008**.
6. A.S. Cuevas, C.A. Arancibia-Bulnes, B. Serrano, *International Journal of Chemical Reactor Engineering*, **2007**, *5,* A58.
7. Ch. Gottschalk, J.A. Libra, A. Saupe, "Ozonation of Water and Waste Water"- 2nd edition, Wiley-VCH Verlag GmbH, Weinheim, **2010**.
8. W.H. Glaze,Y. Lay, J.W. Kang, *Ind. Eng. Chem. Res.*,**1995**, *34*, 2314.
9. K.A. Hoffmann, S.T. Chiang, "Computational Fluid Dynamics", vol **3**, 4th edition, Engineering Education System, Wichita, Kansas, USA, **2000**.
10. P.R. Harris, J.S. Dranoff, *AIChE Journal*, **1965**, *11*, 497.
11. K. Ikehata, M.G. El-Din, *Ozone: Science & Engineering*, **2004**, *26:4,* 327**.**
12. S.M. Jacob, J.S. Dranoff, *Chem. Eng. Prog. Symp. Ser.*, 1**966**, *62*, 47.
13. S.M. Jacob, J.S. Dranoff, *Chem. Eng. Prog. Symp. Ser.*, **1968**, *64*, 54.
14. Leifer A., "The Kinetics of Environmental Aquatic Photochemistry: Theory and Practice", American Chemical Society, New York, **1998**.
15. R.W. Lewis, P. Nithiarasu, K.N. Seetharamu, "Fundamentals of the Finite Element Method for Heat and Fluid Flow", John Wiley & Sons, Ltd, Chichester, UK, **2005**.
16. S. Ulinici, G. Vlad, L. Suciu, *Environmental Engineering and Management Journal*, **2010**, *9:5*, 637.
17. B.A. Wols, J.A.M.H. Hofman, E.F. Beerendonk, W.J.S. Uijtewaal, J.C. Van Dijk, *AicHE Journal*, **2010,** *57:1*, 193.